Journal of Manufacturing Processes 62 (2021) 806–816

Contents lists available at ScienceDirect

Journal of Manufacturing Processes

journal homepage: www.elsevier.com/locate/manpro

Technical Paper

Online tool condition monitoring for ultrasonic metal welding via sensor fusion and machine learning

Qasim Nazir, Chenhui Shao *

Department of Mechanical Science and Engineering, University of Illinois at Urbana-Champaign, 1206 W. Green St, Urbana, IL 61801, USA

ARTICLE INFO

Keywords:
Ultrasonic metal welding
Tool condition monitoring
Machine learning
Sensor fusion
Maintenance
Quality control

ABSTRACT

In ultrasonic metal welding (UMW), tool wear significantly affects the weld quality and tool maintenance constitutes a substantial part of production cost. Thus, tool condition monitoring (TCM) is crucial for UMW. Despite extensive literature focusing on TCM for other manufacturing processes, limited studies are available on TCM for UMW. Existing TCM methods for UMW require offline high-resolution measurement of tool surface profiles, which leads to undesirable production downtime and delayed decision-making. This paper proposes a completely online TCM system for UMW using sensor fusion and machine learning (ML) techniques. A data acquisition (DAQ) system is designed and implemented to obtain in-situ sensing signals during welding processes. A large feature pool is then extracted from the sensing signals. A subset of features are selected and subsequently used by ML-based classification models. A variety of classification models are trained, validated, and tested using experimental data. The best-performing classification models can achieve close to 100% classification accuracy for both training and test datasets. The proposed TCM system not only provides real-time TCM for UMW but also can support optimal decision-making in tool maintenance. The TCM system can be extended to predict remaining useful life (RUL) of tools and integrated with a controller to adjust welding parameters accordingly.

1. Introduction

UMW is an important manufacturing process used for joining multi-layer, thin and conductive metals using high frequency oscillations [1–5]. A notable industrial application of UMW is battery-tab joining in the manufacturing of lithium-ion battery packs for electrical vehicles [3,5]. UMW has also been successfully employed for automotive body construction [1,6], joining of hybrid heat exchangers [5,7,8], and electronic packaging [9,10]. Fig. 1 shows the schematic of a typical ultrasonic metal welder. The welder has two main parts: (1) **Actuator** which consists of moving parts such as transducer, booster, horn and anvil; and (2) **Controller** which controls the movement of the actuator components.

The surfaces of typical welder tools (i.e., horn and anvil) consist of many pyramid-shape knurls [11–13]. UMW tools wear out quickly in production, mostly in the form of material loss [11,12]. There exist relative movements not only between horn and top sheet but also between bottom sheet and anvil. These relative movements are believed to be a major cause of tool wear [11,14]. Tool maintenance is reported to constitute a significant portion of production cost in battery pack manufacturing [11,12]. Tool maintenance related costs can be divided into two major categories [11]: (1) costs induced by production downtime and (2) costs for reworking, or refurbishing worn tools.

In UMW, tool wear significantly affects the weld quality [12,15] and as a result the overall product quality. For example, a battery pack used by Chevy Volt consists of hundreds of battery cells, which are joined primarily using UMW. A single low-quality joint can result in the failure of the entire battery pack. Therefore, vehicle battery manufacturing has a strict requirement for joint quality to avoid high production losses, and consequently employs a conservative tool maintenance strategy. In the absence of a TCM system, a conservative tool replacement approach is used [12]. The number of welds is used as a measure of tool wear and a tool is replaced once a pre-determined limit is reached. This approach is simple to implement but cannot account for machine-to-machine or tool-to-tool variability. Thus, it may sacrifice some useful tool life and lead to increased production cost. Furthermore, existing TCM methods for UMW require frequent high-resolution measurement of tool surface profiles to estimate tool wear development [12]. This approach is

* Corresponding author.
E-mail address: chshao@illinois.edu (C. Shao).
URL: https://mechanical.illinois.edu/directory/faculty/chshao (C. Shao).

https://doi.org/10.1016/j.jmapro.2020.12.050
Received 25 August 2020; Received in revised form 17 December 2020; Accepted 17 December 2020
Available online 19 January 2021
1526-6125/

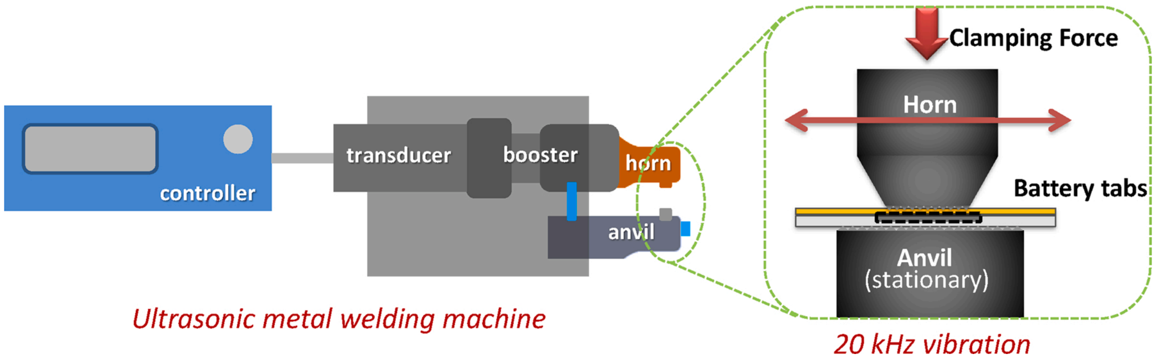

Fig. 1. Schematic of the ultrasonic metal welder [5].

cumbersome from operation point of view and increases production downtime, thereby increasing production cost. As a result, an online TCM system is critically required to ensure joint quality and reduce production cost.

To address these issues, this paper proposes a completely online TCM system for UMW using sensor fusion and ML techniques. An experimental case study is used to validate this methodology. The main contributions of this paper include the following:

- Design and implementation of an automated DAQ system to obtain in-situ sensing signals during welding processes.
- Extraction and selection of useful features for distinguishing different tool conditions in UMW.
- Training, validation, and testing of a variety of classification models using experimental data.
- Discussion about the relationship between useful features and tool wear mechanism in UMW.
- Identification of useful sensing signals for TCM in UMW. Displacement and acoustic emission (AE) signals proved to be more useful than others.
- Future recommendations to extend the proposed TCM system for prediction of RUL of tools and integration with a controller to adjust welding parameters accordingly.

The remainder of the paper is organized as follows: Section 2 presents a literature review of existing TCM methods. Section 3 introduces the proposed methodology for developing an online TCM system and explains each step in detail using an experimental case study. Section 4 discusses the experimental results. Section 5 provides conclusions and recommendations for future work.

2. Literature review

TCM has been an active area of research in the past few decades due to its importance in the manufacturing industry [16]. In particular, TCM for machining including milling [17–21], grinding [22], turning [22,23], and atomic force microscope tip-based nanomachining [24] as well as forming [23,25,26] processes has received substantial attention. TCM methods for machining processes that have been practiced and described in the literature are summarized and discussed by Abellan-Nebot and Subirón [16], Zhou and Xue [17] and Mohanraj et al. [18]. TCM has also been studied for forming processes especially in extrusion and forging processes and online TCM systems were developed [25,26].

In general, TCM techniques can be categorized into two groups [12]: direct and indirect methods. Direct methods rely on direct measurements obtained by visual inspection, 3D-scanning, or computer vision for determining tool wear, e.g., [18]. However, direct methods are not preferred since they are cumbersome and may increase production downtime and cost.

Indirect methods utilize data from the sensors attached to the machine to infer the tool status using a decision-making model. Indirect methods are often preferred because they do not involve any direct tool measurements or substantial production downtime. Indirect methods can further be categorized into model-based [18,27] and data-driven methods [16,28]. Model-based methods require in-depth knowledge of the tool wear mechanism for a manufacturing process. The tool wear mechanism depends on varying process parameters and conditions [29]. This makes it difficult to develop an effective TCM system for some manufacturing processes. On the other hand, data-driven methods use artificial intelligence techniques such as ML or pattern recognition methods [29]. These algorithms rely on past data and do not need to be explicitly programmed. This makes them quite popular for TCM applications in manufacturing.

A comprehensive review on indirect data-driven TCM methods utilizing artificial intelligence techniques is presented in [16]. A typical workflow for developing an indirect TCM system includes the following key steps [16]: (i) sensor selection, (ii) signal pre-processing, (iii) feature generation, (iv) feature selection, and (v) decision-making algorithm. Relevant features are calculated from sensing signals to represent data in lower dimensions. In general, features can be categorized into three groups: (1) time domain, (2) frequency domain, and (3) time-frequency domain. Extensive literature about feature generation methods can be found in [16,30]. Feature selection techniques are then used to select a parsimonious set of features [31–33]. There exists a wide range of algorithms for decision-making [18] such as fuzzy logic systems, Bayesian networks, decision trees, support vector machine (SVM), and artificial neural networks (ANN). Recent trends are shifting towards the use of deep learning techniques which combine feature generation and model training steps in a single process [19]. Some attempts have also been made for adaptive process control using sensing signals [34–36].

A number of studies have been reported on data-driven TCM methods, such as [19–23,25,26]. Zheng and Lin [19] used time-frequency images of cutting force signals and convolutional neural networks for TCM in machining process. Drouillet et al. [20] developed neural networks to predict RUL using the machine spindle power values in a milling process. Zhou and Xue [21] developed a multi-sensor fusion method for TCM in milling, in which a kernel-based extreme learning machine and a modified genetic algorithm were used for parameter search. Zhang and Shin [22] developed a multi-modal system for predicting tool wear, detecting chatter and tool chipping in turning processes using the same set of sensing signals. Bhuiyan et al. [23] explored the application of AE sensor to investigate the frequency of tool wear and plastic deformation in TCM for turning processes. Kong and Nahavandi [25] and Kim [26] used multiple sensing signals and decision-making algorithms such as principal curve fitting and neural networks for TCM in forging processes.

Despite extensive literature focusing on online (or indirect) TCM system development for other manufacturing processes, limited studies have been reported on online TCM for UMW. Developing an online TCM

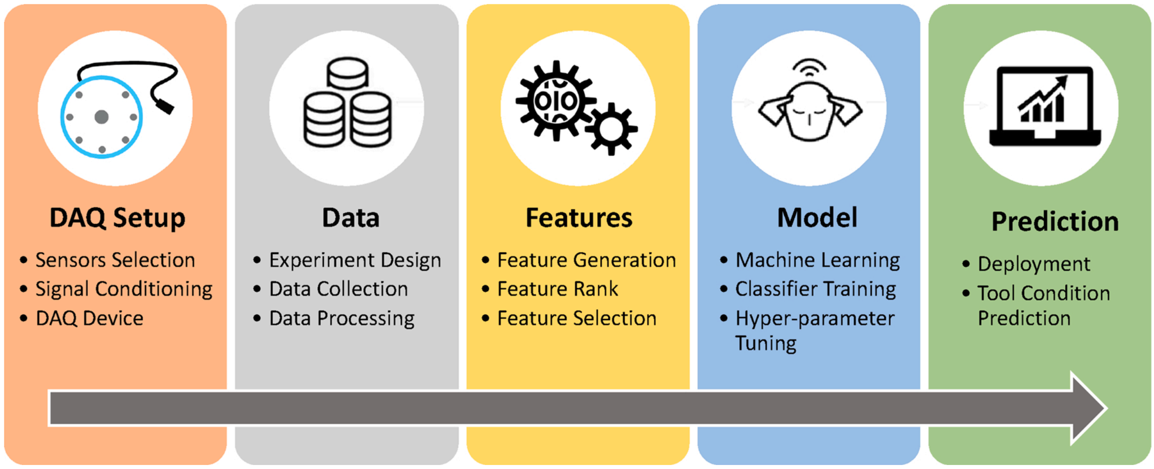

Fig. 2. Schematic description of the online TCM system for UMW.

system for UMW is more challenging than other processes such as machining and forming. UMW has characteristics of high oscillation frequency (around 20 kHz) and short welding cycle (typically below 1 s) [1,2]. Moreover, the UMW tools have complex shapes [12] and the process itself has not been thoroughly understood.

Some previous research [11,12,15] has been reported on the development of direct TCM systems for UMW. These methods rely on manual tool surface measurement and none of them is completely online. The tool wear progression in UMW was characterized by comparing tools at four different tool wear stages [11]. For this purpose, the tool surfaces were measured using a high-resolution 3D surface measurement system. An impression method was used to measure tool surface without removing the tool from the welder [12], and features were then calculated from cross-sectional tool surface profiles for TCM. A high-order decomposition method is presented in [15] for TCM in UMW.

Some studies [35,37] have also been reported in the literature that involve the usage of sensing signals for online quality monitoring in UMW. An online monitoring system was developed for weld-quality prediction in UMW of lithium-ion batteries [37]. Recently, Nong et al. [35] utilized sensing signals for the control of UMW.

To summarize, limited studies are available on TCM for UMW. Existing TCM methods for UMW require offline high-resolution measurement of tool surface profiles, which leads to undesirable production downtime and delayed decision-making. Therefore, there is a strong need for a completely online TCM system for UMW using sensor fusion and ML techniques.

3. Methodology

Fig. 2 presents a schematic description of the proposed online TCM system for UMW. The first stage is the identification of relevant sensors using domain expertise and installation of a DAQ setup. The second stage is to run experiments and collect sensing signals for known tool conditions. The third stage is to reduce the dimensionality of data by extracting and selecting useful features from signals. The fourth stage is the development of classification models. This process is iterative, and involves training, validation and testing of a variety of classification models with various hyper-parameter settings. Once satisfied with the classification performance, the final stage is to deploy the model for online TCM.

3.1. DAQ setup

The first stage is the design and implementation of an automated DAQ system to obtain sensing signals during welding processes. Some of the sensing signals require signal conditioning before being fed to the DAQ device. Four relevant data sources were identified using UMW domain knowledge as shown in Fig. 3 and are briefly described below.

1. **Power Signal:** It provides a profile of instantaneous power used by the welder during a welding process. This signal is directly obtained from the welder controller.
2. **Displacement Signal:** It provides a profile of instantaneous vertical displacement of the horn. This signal is directly obtained from the linear velocity displacement transducer (LVDT) sensor installed in the welder actuator.
3. **Sound Signal:** A microphone is placed close to the actuator to obtain the sound signal. A pre-amplifier is used to amplify the sound signal before the signal is transmitted to the DAQ device.
4. **AE Signal:** An AE sensor is attached to the anvil to record acoustic emissions generated during the welding process. A pre-amplifier is used to amplify the AE signal.

3.2. Data collection

The welder has two main tools, namely, a horn and an anvil, whose conditions need to be monitored. In this study, we have two horn conditions, i.e., new and worn, and two anvil conditions, i.e., new and worn,

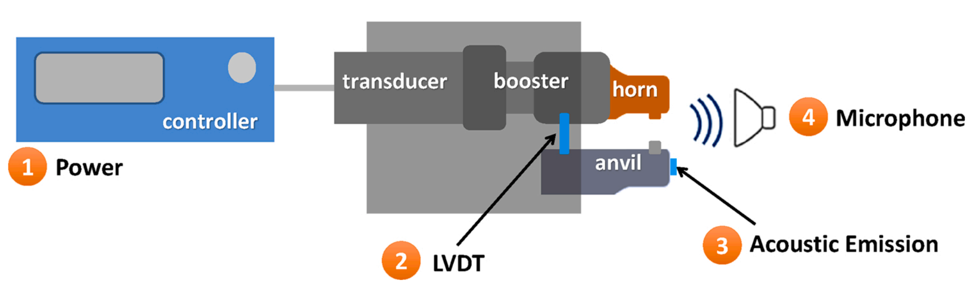

Fig. 3. Schematic of the sensors used for online TCM.

Table 1
Labels assigned to tool condition combinations.

Label	Horn condition	Anvil condition
0	New	New
1	New	Worn
2	Worn	New
3	Worn	Worn

which result in four combined tool conditions as listed in Table 1.

The tool surfaces were also measured using Keyence VK-X1000, which is a high-resolution 3D surface measurement system. A comparison of tool conditions for horn and anvil is shown in Figs. 4 and 5 .

Using the process parameters listed in Table 2, 50 samples were welded for each tool condition, and corresponding sensing signals were recorded. The signals were pre-processed to remove noise and trimmed to extract data corresponding to the weld-duration only.

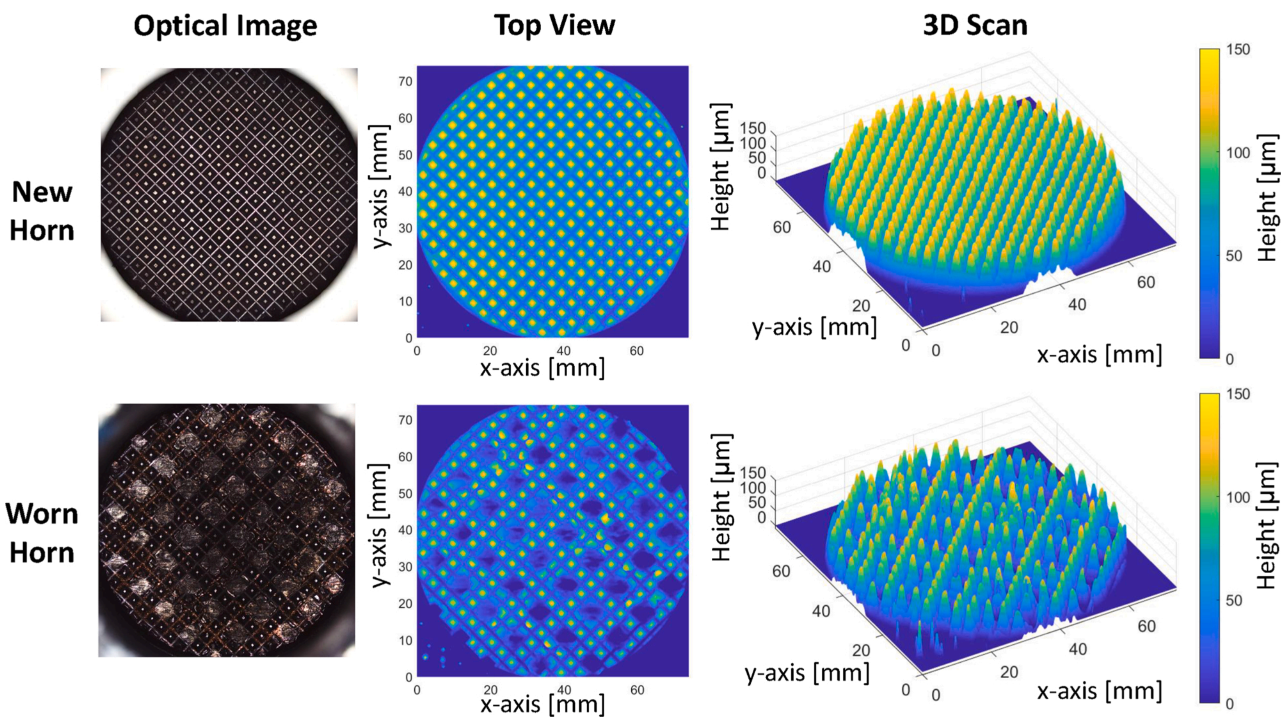

Fig. 4. Comparison of new and worn horns.

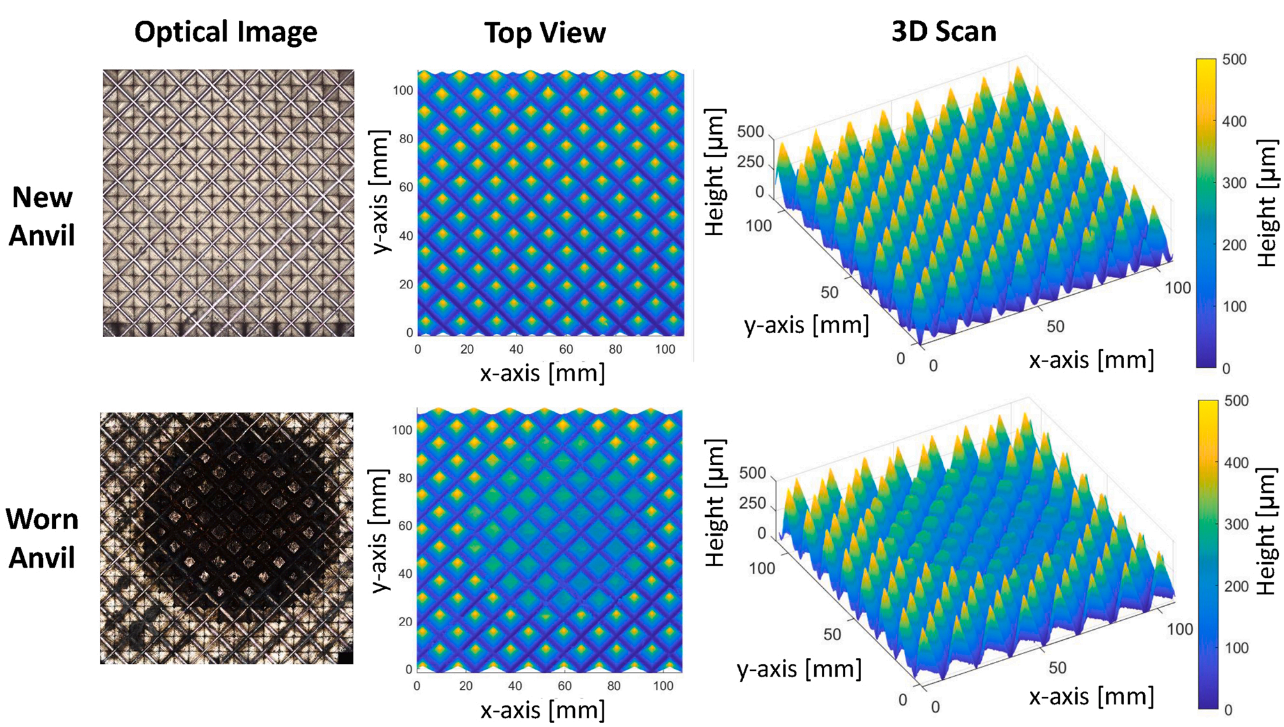

Fig. 5. Comparison of new and worn anvils.

Table 2
UMW process parameters used for data collection.

	Parameter	Value
Weld coupon	Material	Copper
	Dimensions	50.8 mm × 25.4 mm × 0.2032 mm
Controller settings	Control mode	Time mode
	Weld time	0.5 s
	Pressure	40 Psi
	Amplitude	45 μm
DAQ settings	Trigger mode	On
	Signal duration	2 s
	Sample rate	250 kHz

Fig. 6 shows all sensing signals for each tool condition. AE and sound signals are visualized in frequency domain in Fig. 7 because of their periodic nature. This visualization helps in understanding the overall distribution of sensing signals and identifying the differences in signals across different tool conditions. It can be observed that sensing signals contain rich information about the process; however, it is difficult to visually differentiate among tool conditions. There exists strong variations within each tool condition, leading to substantial overlap between tool conditions. The worn/worn tool condition shows the strongest within-class variation, indicating poor process robustness.

The variation in signals and lack of robustness in UMW process makes it challenging to develop an online TCM system. Simple features might not be sufficient to develop an effective TCM system. Therefore, extensive feature engineering is required to generate a large feature pool from sensing signals and then select the most useful features using feature selection techniques.

3.3. Feature engineering

3.3.1. Feature generation

As observed in Figs. 6 and 7, sensing signals contain rich information about the process and the tool condition. However, being unstructured and high dimensional, the sensing signals cannot be directly used to train traditional classification algorithms. Therefore, it is required to reduce data dimensionality and extract useful features from the signals. Features can be broadly divided into two main categories.

1. **Time-Domain Features**
   Signal statistics such as mean, median, standard deviation, kurtosis, skewness, root mean square, maximum, and minimum can be

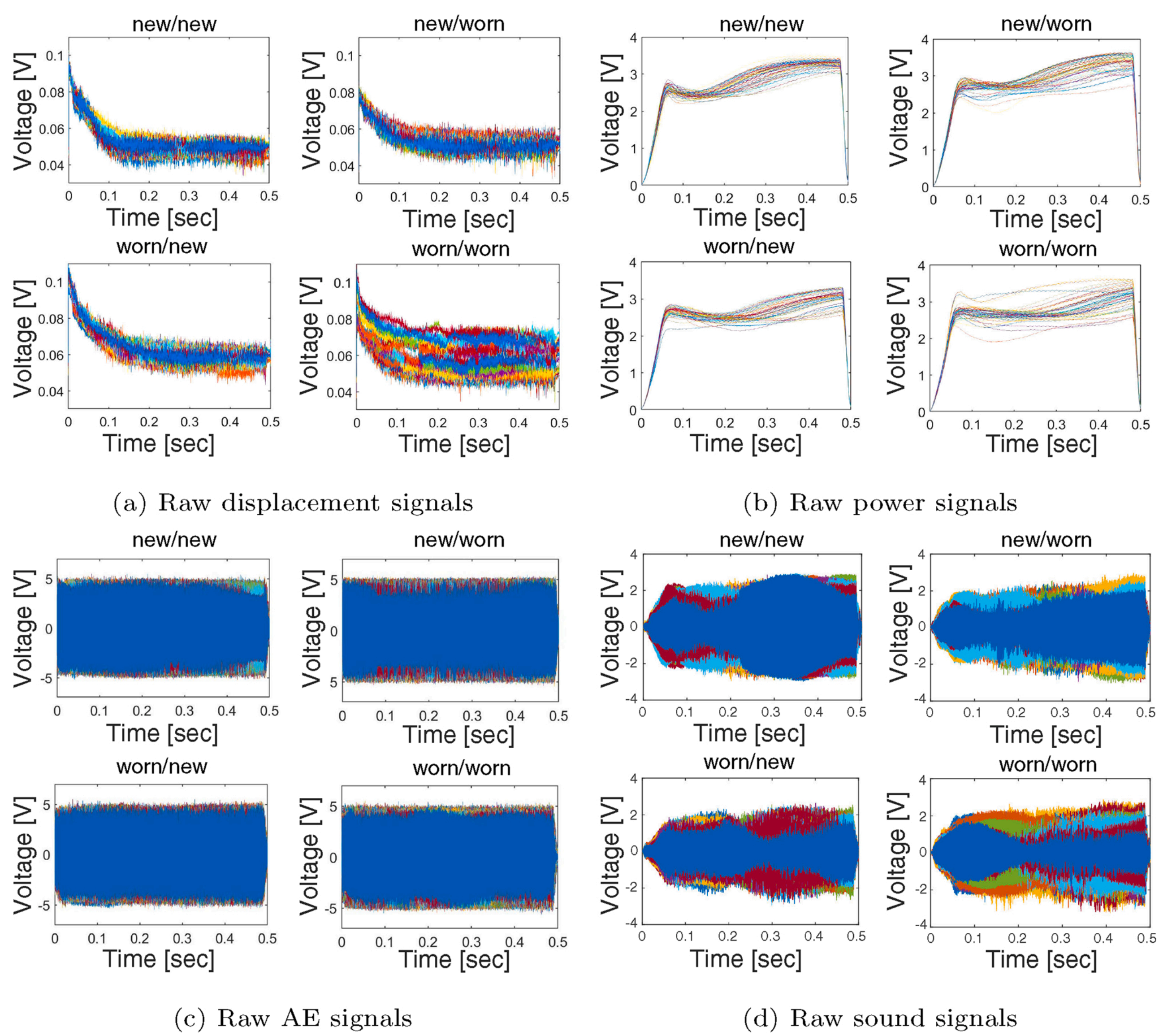

Fig. 6. Raw sensing signals for tool conditions horn/anvil.

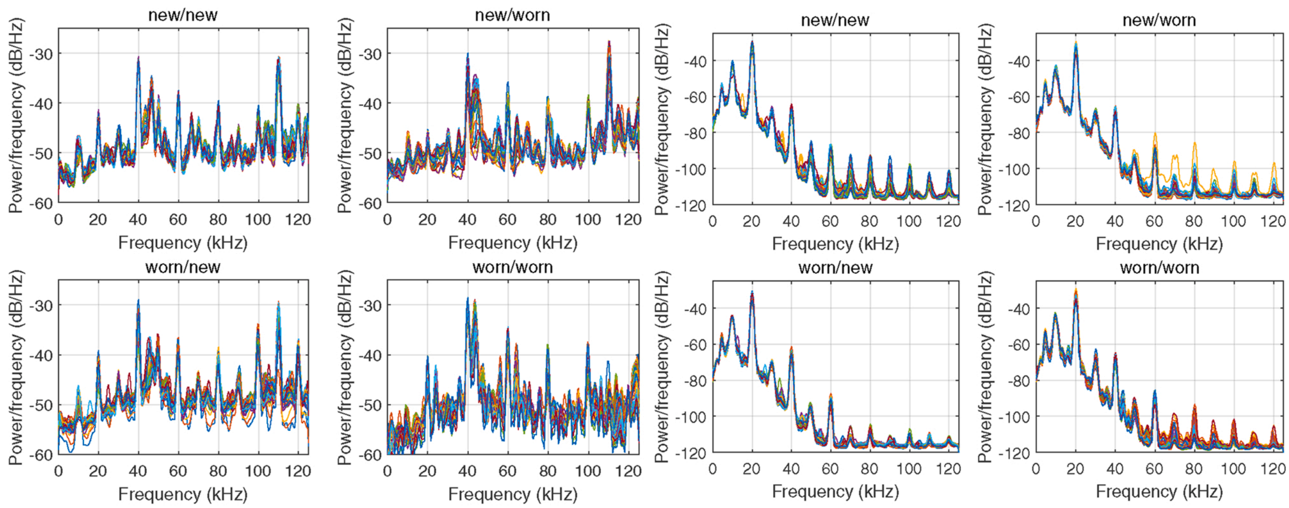

(a) PSD of AE signals (b) PSD of sound signals

Fig. 7. PSD of AE and sound signals for tool conditions horn/anvil.

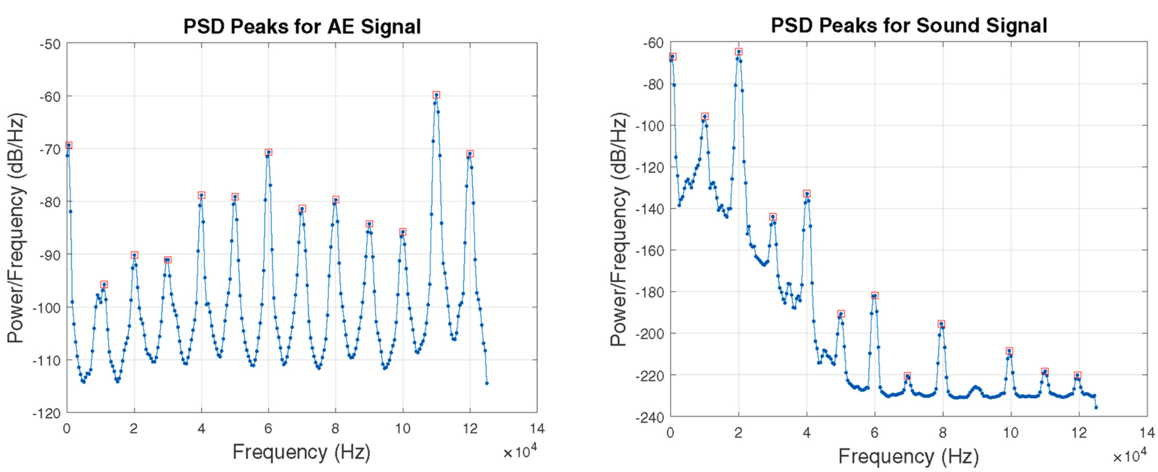

Fig. 8. Frequency domain features extracted from `PSD` of sensing signals.

potentially useful features. Other useful features are calculated using domain knowledge such as the welding energy which is the area under the power curve, and the change in displacement.

2. **Frequency-Domain Features**

   Frequency-domain representation of a signal is particularly useful in the case of periodic signals such as sound and AE. It gives information about dominant frequencies and is an effective way to represent signals in lower dimensions. First ten peaks from the PSD of AE and sound signals are used as features as shown in Fig. 8.

The UMW controller also saves parameters such as total energy and power utilized in log files during the welding process. These parameters are also included as potential features. The complete list of features along with their descriptions can be found in Table 3.

3.3.2. *Feature selection*

In total, 97 features are calculated from sensing signals but not all of them are useful in classification. Feature selection is often used to select a subset of useful features and can be broadly categorized into three types: [32,33] (1) wrapper methods, (2) filter methods, and (3) embedded methods. It is desirable to only retain the most useful features without discarding possibly useful information about the welding process. In this study, the most useful features are selected using a feature selection procedure that is explained as follows. First, features with very low variance, i.e., features that have the same or very close values in all samples, are discarded. Then, we use multiple feature selection methods that are available in the scikit-learn machine learning library to select 10 features each. These methods include (1) SelectKbest, (2) SelectFromModel, (3) FeatureImportance, and (4) recursive feature elimination with cross-validation (RFECV). Interested readers are referred to [38] for details. The final feature set is generated by taking union of feature sets obtained in the previous step.

3.3.3. *Feature subsets*

There are different sources for the extracted features as listed in Table 3. For online TCM system development, one approach is to utilize all the sensing signals also known as sensor fusion and create a large feature pool to be used by ML-based classification models. An alternative approach is to utilize features only from individual sensing signals. Thus depending on the sensing signals used, we can have various feature subsets to be used for classification model development as listed in Table 4. The sensor fusion feature set includes features from all the sensing signals. Other feature subsets are named by the source of the sensing signal.

It is interesting to compare the performance of classification models developed using different feature subsets. It is expected that the model

Table 3
List of features.

Source	Feature	Description
Log files	Energy	Energy consumed during welding
	Power	Peak power during welding
	PreHeight	Horn height before weld
	PostHeight	Horn height after weld
	ChangeHeight	Change in horn height
AE Signal	Amean	Mean of AE signal
	Amedian	Median of AE signal
	Astd	Standard deviation of AE signal
	Akurtosis	Kurtosis of AE signal
	Askewness	Skewness of AE signal
	Arms	Root mean square value of AE signal
	Amax	Maximum value of AE signal
	Amin	Minimum value of AE signal
	Arange	Range of AE signal
	Aentropy	Entropy of AE signal
	Apsd_pk[n]	The nth peak from psd of AE signal. $n \in [\![1, 10]\!]$
	Apsd_f[n]	Frequency at the nth peak of psd. $n \in [\![1, 10]\!]$
	Apsd_meanfreq	Mean frequency of psd
Displacement signal	Dmean	Mean of displacement signal
	Dmedian	Median of displacement signal
	Dstd	Standard deviation of displacement signal
	Dkurtosis	Kurtosis of displacement signal
	Dskewness	Skewness of displacement signal
	Drms	Root mean square value of displacement signal
	Dmax	Maximum value of displacement signal
	Dmin	Minimum value of displacement signal
	Disp_initial	Displacement of horn at start of weld
	Disp_final	Displacement of horn at end of weld
	Disp_change	Change in displacement
	Dpsd_pk[n]	The nth peak from psd of displacement signal. $n \in [\![1, 5]\!]$
	Dpsd_f[n]	Frequency at the nth peak of psd. $n \in [\![1, 5]\!]$
	Dpsd_meanfreq	Mean frequency of psd
Power signal	Pmean	Mean of power signal
	Pmedian	Median of power signal
	Pstd	Standard deviation of power signal
	Pkurtosis	Kurtosis of power signal
	Pskewness	Skewness of power signal
	Prms	Root mean square value of power signal
	Pmax	Maximum value of power signal
	Pmin	Minimum value of power signal
	PEnergy	Area under power signal curve
Sound signal	Smean	Mean of sound signal
	Smedian	Median of sound signal
	Sstd	Standard deviation of sound signal
	Skurtosis	Kurtosis of sound signal
	Sskewness	Skewness of sound signal
	Srms	Root mean square value of sound signal
	Smax	Maximum value of sound signal
	Smin	Minimum value of sound signal
	Srange	Range of sound signal
	Sentropy	Entropy of sound signal
	Spsd_pk[n]	The nth peak from psd of sound signal. $n \in [\![1, 10]\!]$
	Spsd_f[n]	Frequency at the nth peak of psd. $n \in [\![1, 10]\!]$
	Spsd_meanfreq	Mean frequency of psd

developed using sensor fusion should give the best performance since it uses the most information about the tool condition. However, hardware resources can be minimized if a model developed using individual sensing signals can provide comparable results.

Therefore, the feature selection process explained in Section 3.3.2 is repeated for each feature subset. Table 4 summarizes the feature count and selected features for each subset.

Table 4
List of features selected for classification model training.

Feature set	Count	Selected features
Sensor fusion	15	Disp_initial, Aentropy, Astd, Dskewness, Arms, Apsd_pk9, Apsd_pk6, Dpsd_pk2, Dentropy, Dpsd_pk3, Disp_change, Apsd_pk7, Disp_final, Dmean, Akurtosis
Log features	4	Energy, Power, PreHeight, PostHeight, ChangeHeight
AE features	14	Apsd_pk6, Apsd_pk7, Apsd_pk9, Apsd_f2, Apsd_pk5, Astd, Arms, Amean, Aentropy, Apsd_pk1, Apsd_pk2, Apsd_pk3, Arange, Akurtosis
Displacement features	16	Dpsd_f3, Dpsd_pk2, Dskewness, Dkurtosis, Dpsd_pk3, Drange, Dmean, Disp_final, Dstd, Dpsd_meanfreq, Dpsd_f5, Dentropy, Disp_change, Dpsd_pk4, Dmedian, Disp_initial
Power features	10	Pskewness, Pentropy, Prms, Pkurtosis, Pstd, Pmedian, Pmean, Prange, Energy, Pmax
Sound features	15	Spsd_pk3, Spsd_pk10, Smin, Spsd_pk8, Spsd_f8, Srms, Spsd_pk9, Sstd, Sskewness, Spsd_pk2, Spsd_f10, Spsd_f5, Smean, Spsd_pk5, Spsd_pk6

Table 5
Results for best-performing models among the various classification models that were trained and tested on different feature subsets using 5-fold cross validation.

Feature set	Classification models	5-Fold cross validation			
		Train Mean	Train Std	Val Mean	Val Std
Sensor fusion	QDA	100.0	0.0	99.50	1.00
	SVM linear	100.0	0.0	99.50	1.00
	KNN	100.0	0.0	99.00	2.00
Log features	SVM RBF	94.25	0.47	82.50	5.70
	QDA	86.00	1.16	80.00	5.70
	Naive Bayes	83.12	2.34	79.00	4.36
AE features	Extra tree	99.50	0.47	97.00	2.45
	Logistic regression	100.0	0	97.00	3.67
	LDA	99.12	0.50	97.00	6.00
Displacement features	LDA	100.0	0.0	99.50	1.00
	SVM linear	100.0	0.0	99.00	1.22
	Logistic regression	99.75	0.31	99.00	1.22
Power features	LDA	88.88	1.55	83.50	10.79
	SVM RBF	98.38	0.50	78.50	9.43
	QDA	95.12	1.08	77.50	10.0
Sound features	Gradient boosting	100.0	0.00	86.50	8.31
	Extra tree	100.0	0.00	85.00	10.25
	Random forest	98.62	0.73	81.00	11.14

3.4. Classification model development

The dataset is used to train and test candidate ML classification models using 5-fold cross validation. The candidate models include linear discriminant analysis (LDA), quadratic discriminant analysis (QDA), logistic regression, K-nearest neighbors (KNN), SVM with different kernels (linear, polynomial, and radial basis function – RBF), naive Bayes, decision tree, random forest, gradient boosting, and extra tree.

Hyper-parameters of classification algorithms influence the classification performance and thus need to be carefully tuned. Considering the wide range of ML algorithms and their hyper-parameters, it is difficult and computationally expensive to find a globally optimal solution. Therefore, an iterative approach is used for model training along with hyper-parameter tuning until satisfactory results are achieved. Similar

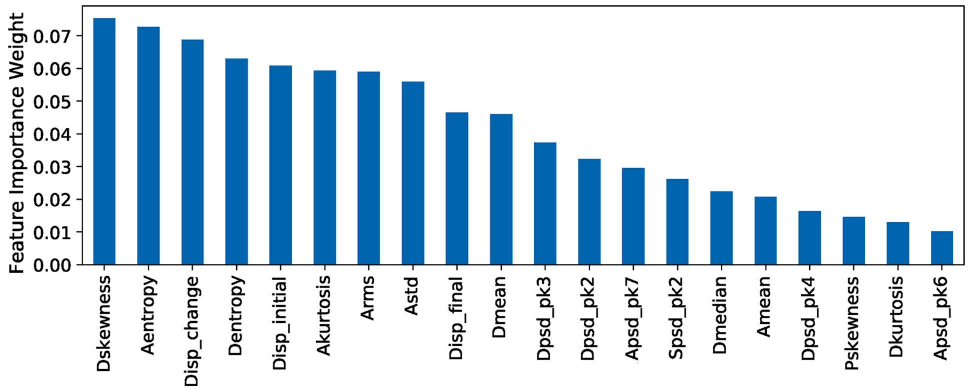

Fig. 9. Top 20 features ranked in order of their usefulness for class labels differentiation.

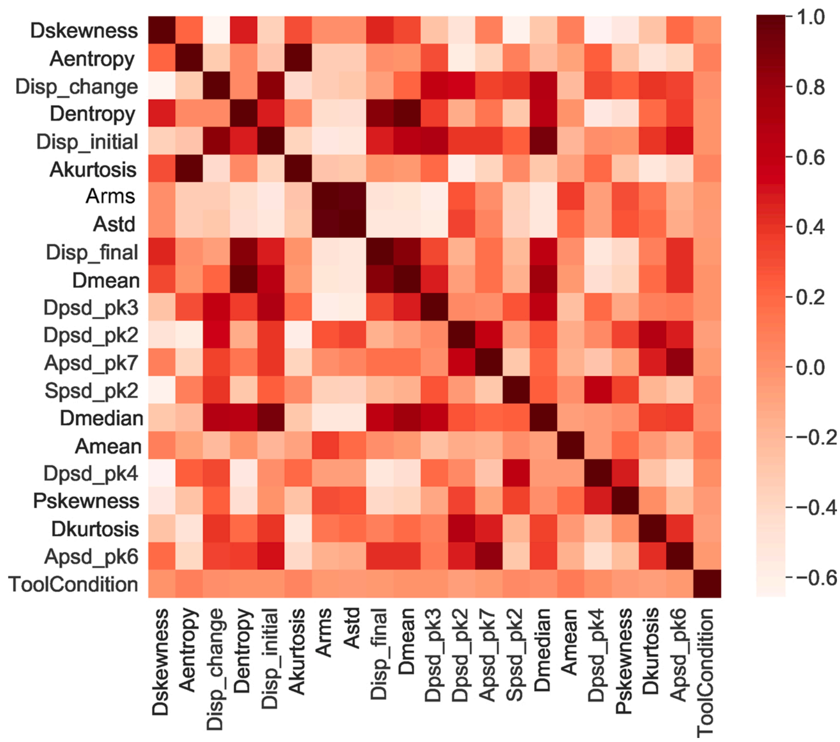

Fig. 10. Heat map of top 20 features.

to the feature selection process, the classification model development process is repeated for each feature subset. The results from the best-performing classification models for each feature subset are summarized in Table 5.

4. Discussion

Promising results were achieved by the developed online TCM system in the experimental case study. As listed in Table 5, the best-performing models achieve close to 100% accuracy for both training and validation datasets.

Comparison of classification accuracy results from different feature subsets, as listed in Table 5, leads to some interesting observations. Displacement and AE signals prove to be the most useful in predicting tool conditions. Power and sound signals give reasonable results but are not as good as the other two signals. Results obtained from the displacement features subset are comparable to the results of sensor fusion. Thus, for this case study with four tool conditions, a good TCM system can be developed by using a displacement signal alone instead of using sensor fusion. This will not only save hardware resources but will also result in faster data processing when deployed for real-time TCM.

Features are also ranked by their importance in each feature subset. In the case of sensor fusion, the most useful features come from displacement and AE signals as shown in Fig. 9. This again supports the importance of these two signals.

Fig. 11 shows pair-plots of the most useful features from AE and displacement signals. From the scatter plots, it can be observed that important features can differentiate tool conditions well. These features have good between-class separability and small variability within each class. Fig. 12 shows pair-plots of some useful features from power and sound signals. It can be observed that these features provide reasonable separability between classes but they are not as good as the features from the other two signals.

From the heat-map of features shown in Fig. 10, it can be seen that some features are correlated to each other even though they are good in differentiating among classes. These features are redundant and add similar information to the classification model. Some of these features can be discarded to make the algorithm more efficient.

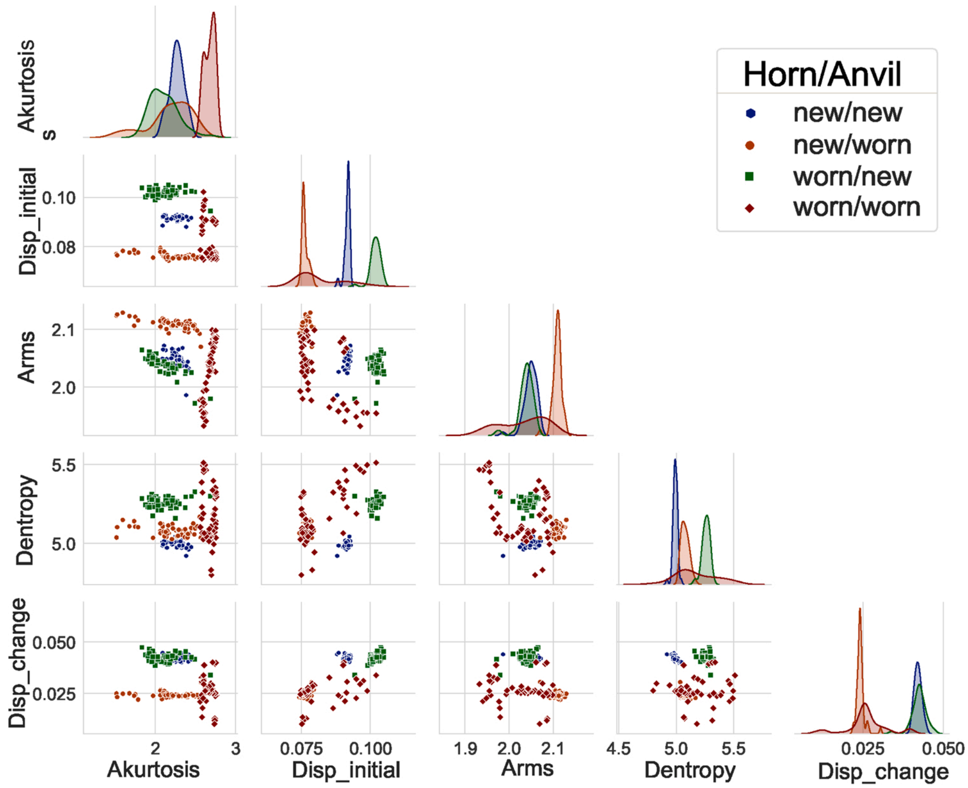

Fig. 11. Scatter plot of top 5 features that were extracted from AE and displacement signals.

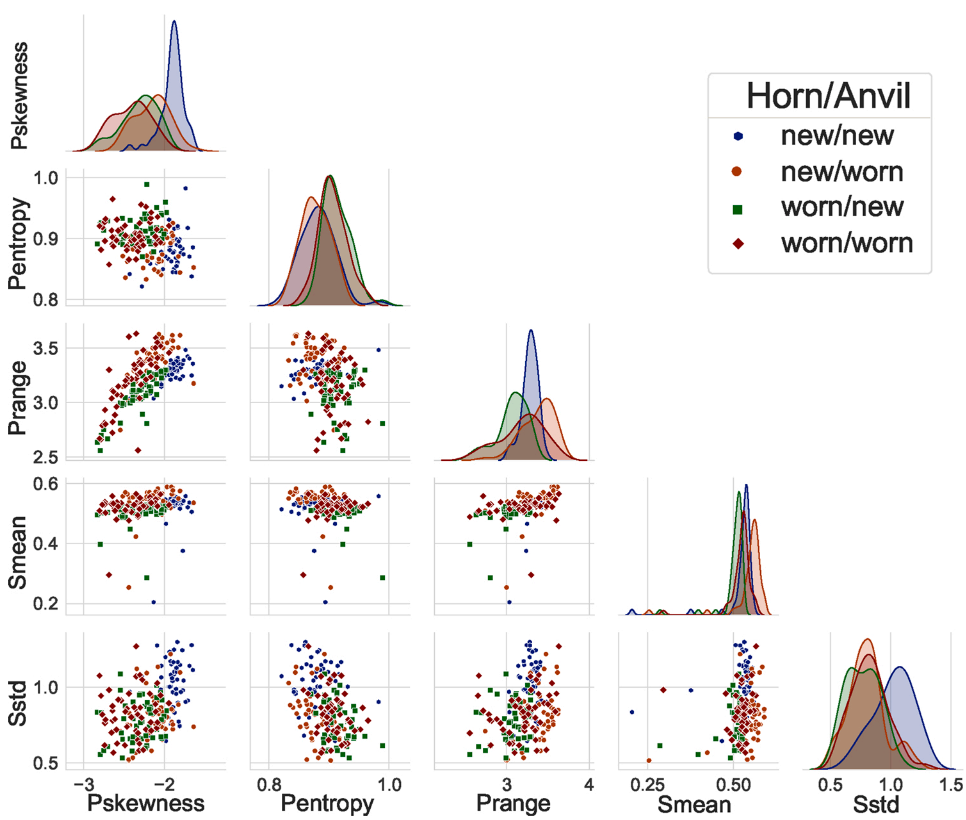

Fig. 12. Scatter plot of top 5 features that were extracted from power and sound signals.

The displacement signal provides some insights in understanding the tool wear mechanism. The signal represents the instantaneous distance between the horn and the anvil. In particular, the initial displacement of horn is quite helpful in understanding the process. Fig. 11shows the distribution of Disp_initial. For new tools, this feature has nominal values. As the anvil surface gets worn out, the weld coupons are placed at lower height and Disp_initial will have lower values. Disp_initial has higher values when a worn horn is used. A large variation in Disp_initial is observed when both horn and anvil are worn out.

Disp_change is the difference between the final and initial displacements of the horn. In other words, it represents the change in thickness of weld coupon during the welding process. It is also helpful for differentiating tool conditions. A larger value of Disp_change is observed for the new anvil as compared to the worn anvil. This means that the condition of the anvil primarily affects the change in thickness of weld coupon.

Dentropy is another useful feature. A larger spread in Dentropy values is observed when both the horn and the anvil are worn. It is a useful feature for distinguishing the other three tool conditions from each other because good separability is observed in Fig. 12.

Moreover, several features from the AE signal proved to be useful as shown in Fig. 9. Some statistical features include Aentropy, Akurtosis, Arms, Astd, and Amean. There were some frequency-domain features as well such as Apsd_pk7 and Apsd_pk6. While it is difficult to interpret their physical meaning, they can distinguish tool conditions effectively. This indicates that the tool wear mechanism is challenging to fully understand and the proposed TCM system can provide essential information that is not easily obtainable using physical knowledge about UMW.

5. Conclusion and future work

Despite significant research work done in the area of TCM, limited research exists on the TCM of UMW. Some studies have been performed to develop TCM systems for UMW, but the existing methods require a high-resolution measurement of tool surface profiles, which leads to undesirable production downtime and delayed decision-making. This research developed a completely online TCM system for UMW using sensor fusion and ML techniques. A DAQ system was designed and implemented to obtain multiple sensor signals including AE, displacement, power, and sound signals during the welding process. A subset of monitoring features were selected from a large feature pool and subsequently used by classification models. Experimental data was recorded for four tool conditions and used to test the performance of the developed classifiers. The best classifiers achieved accuracy close to 100% and their performance was very stable. AE and displacement signals proved to be very useful in recognizing the four tool conditions.

The TCM system only classifies the tool condition but does not provide any information about RUL of tools. One future research topic can be focused on developing an online system for RUL prediction. For this purpose, it is required to record sensing signals for the complete lifecycle of a tool. Once we have data for a sufficient number of tools, an RUL prediction algorithm can be developed and integrated with the TCM system.

Another interesting direction is to model the relationships between tool conditions, weld quality and welding parameters such as pressure, amplitude, energy and weld time. Response surface models can be developed to characterize these relationships. These models along with sensing signals can then be used to control the UMW process and enhance weld quality when worn tool conditions are present, thus increasing the tool service life and reducing the production cost.

Declaration of Competing Interest

The authors report no declarations of interest.

Acknowledgements

This research has been supported by the National Science Foundation under Grant No. 1944345.

References

[1] Ni Z, Ye F. Ultrasonic spot welding of aluminum alloys: a review. J Manuf Process 2018;35:580–94.
[2] Ni Z, Yang J, Li S, Wang X, Ye F. A review on ultrasonic spot welding of copper alloys. Mater Sci Technol 2019:1–20.
[3] Shawn Lee S, Shao C, Hyung Kim T, Jack Hu S, Kannatey-Asibu E, Cai WW, et al. Characterization of ultrasonic metal welding by correlating online sensor signals with weld attributes. J Manuf Sci Eng 2014;136(5):1–10.
[4] Satpathy MP, Mishra SB, Sahoo SK. Ultrasonic spot welding of aluminum-copper dissimilar metals: a study on joint strength by experimentation and machine learning techniques. J Manuf Process 2018;33:96–110.
[5] Meng Y, Rajagopal M, Kuntumalla G, Toro R, Zhao H, Chang HC, et al. Multi-objective optimization of peel and shear strengths in ultrasonic metal welding using machine learning-based response surface methodology. Math Biosci Eng 2020;17(6):7411–27.
[6] Zhang C, Chen D, Luo A. Joining 5754 automotive aluminum alloy 2-mm-thick sheets using ultrasonic spot welding. Weld J 2014;93(4):131–8.
[7] Meng Y, Peng D, Nazir Q, Kuntumalla G, Rajagopal MC, Chang HC, et al. Ultrasonic welding of soft polymer and metal: a preliminary study. International manufacturing science and engineering conference, vol. 58752 2019. V002T03A083.
[8] Kuntumalla G, Meng Y, Rajagopal M, Toro R, Zhao H, Chang HC, et al. Joining techniques for novel metal polymer hybrid heat exchangers. ASME international mechanical engineering congress and exposition, vol. 59384 2019. p. V02BT02A018.
[9] Daniels H. Ultrasonic welding. Ultrasonics 1965;3(4):190–6.
[10] Kim J, Jeong B, Chiao M, Lin L. Ultrasonic bonding for mems sealing and packaging. IEEE Trans Adv Packag 2009;32(2):461–7.
[11] Shao C, Guo W, Kim TH, Jin JJ, Hu SJ, Spicer JP, et al. Characterization and monitoring of tool wear in ultrasonic metal welding. 9th international workshop on microfactories 2014:161–9.
[12] Shao C, Hyung Kim T, Jack Hu S, Jin J, Abell JA, Patrick Spicer J, et al. Tool wear monitoring for ultrasonic metal welding of lithium-ion batteries. J Manuf Sci Eng 2016;138(5):1–8.
[13] Yang Y, Shao C. Spatial interpolation for periodic surfaces in manufacturing using a Bessel additive variogram model. J Manuf Sci Eng 2018;140(6).
[14] Shawn Lee S, Hyung Kim T, Jack Hu S, Cai WW, Abell JA. Analysis of weld formation in multilayer ultrasonic metal welding using high-speed images. J Manuf Sci Eng 2015;137(3):1–8.
[15] Zerehsaz Y, Shao C, Jin J. Tool wear monitoring in ultrasonic welding using high-order decomposition. J Intell Manuf 2019;30(2):657–69.
[16] Abellan-Nebot JV, Subirón FR. A review of machining monitoring systems based on artificial intelligence process models. Int J Adv Manuf Technol 2010;47(1–04): 237–57.
[17] Zhou Y, Xue W. Review of tool condition monitoring methods in milling processes. Int J Adv Manuf Technol 2018;96(5–8):2509–23.
[18] Mohanraj T, Shankar S, Rajasekar R, Sakthivel N, Pramanik A. Tool condition monitoring techniques in milling process – a review. J Mater Res Technol 2020;9 (1):1032–42.
[19] Zheng H, Lin J. A deep learning approach for high speed machining tool wear monitoring. 2019 3rd international conference on robotics and automation sciences (ICRAS) 2019:63–8.
[20] Drouillet C, Karandikar J, Nath C, Journeaux A-C, El Mansori M, Kurfess T. Tool life predictions in milling using spindle power with the neural network technique. J Manuf Process 2016;22:161–8.
[21] Zhou Y, Xue W. A multisensor fusion method for tool condition monitoring in milling. Sensors 2018;18(11):3866.
[22] Zhang B, Shin YC. A multimodal intelligent monitoring system for turning processes. J Manuf Process 2018;35:547–58.
[23] Bhuiyan M, Choudhury IA, Dahari M, Nukman Y, Dawal S. Application of acoustic emission sensor to investigate the frequency of tool wear and plastic deformation in tool condition monitoring. Measurement 2016;92:208–17.
[24] Cheng F, Dong J. Monitoring tip-based nanomachining process by time series analysis using support vector machine. J Manuf Process 2019;38:158–66.
[25] Kong LX, Nahavandi S. On-line tool condition monitoring and control system in forging processes. J Mater Process Technol 2002;125:464–70.
[26] Kim J. Online multichannel forging tonnage monitoring and fault pattern discrimination using principal curve. Trans ASME J Manuf Sci Eng 2006;128: 944–50.
[27] Visariya R, Ruparel R, Yadav R. Review of tool condition monitoring methods. Int J Comput Appl 2018;179(37):29–32.
[28] Wu D, Jennings C, Terpenny J, Gao RX, Kumara S. A comparative study on machine learning algorithms for smart manufacturing: tool wear prediction using random forests. J Manuf Sci Eng 2017;139(7):1–8.
[29] Li Z, Liu R, Wu D. Data-driven smart manufacturing: tool wear monitoring with audio signals and machine learning. J Manuf Process 2019;48:66–76.
[30] Banerjee S, Chattopadhyay T, Pal A, Garain U. Automation of feature engineering for iot analytics. ACM SIGBED Rev 2018;15(2):24–30.

[31] Shao C, Paynabar K, Kim TH, Jin JJ, Hu SJ, Spicer JP, et al. Feature selection for manufacturing process monitoring using cross-validation. J Manuf Syst 2013;32 (4):550–5.
[32] Tang J, Alelyani S, Liu H. Feature selection for classification: a review. Data classif: Alg Appl 2014:37.
[33] Omar N, Jusoh F, Ibrahim R, Othman M. Review of feature selection for solving classification problems. J Inform Syst Res Innov 2013;3:64–70.
[34] Swain S, Panigrahi I, Sahoo AK, Panda A. Adaptive tool condition monitoring system: a brief review. Mater Today: Proc 2019:474–8.
[35] Nong L, Shao C, Kim TH, Hu SJ. Improving process robustness in ultrasonic metal welding of lithium-ion batteries. J Manuf Syst 2018;48:45–54.
[36] Liu Y, Zhang Y. Fusing machine algorithm with welder intelligence for adaptive welding robots. J Manuf Process 2017;27:18–25.
[37] Guo W, Shao C, Kim TH, Hu SJ, Jin JJ, Spicer JP, et al. Online process monitoring with near-zero misdetection for ultrasonic welding of lithium-ion batteries: an integration of univariate and multivariate methods. J Manuf Syst 2016;38:141–50.
[38] Feature selection – scikit-learn 0.23.2 documentation. https://scikit-learn.org/stable/modules/feature_selection.html [Accessed 24 July 2020].